

DOUBLE-DIFFERENTIAL SPECTRA OF THE SECONDARY PARTICLES IN THE FRAME OF PRE-EQUILIBRIUM MODEL

© 2010 O. V. Fotina^{1)*}, V. L. Kravchuk^{2),3)}, S. Barlini⁴⁾, F. Gramegna²⁾,
D. O. Eremenko¹⁾, Yu. L. Parfenova¹⁾, S. Yu. Platonov¹⁾, O. A. Yuminov¹⁾,
M. Bruno^{3),5)}, M. D'Agostino^{3),5)}, G. Casini⁴⁾, O. Wieland⁶⁾, A. Bracco⁶⁾, F. Camera⁶⁾

Received December 28, 2009

An approach was developed to describe the double-differential spectra of secondary particles formed in heavy-ions reactions. Griffin model of nonequilibrium processes was used to account for the nonequilibrium stage of the compound system formation. Simulation of de-excitation of the compound system was carried out using the Monte-Carlo method. Analysis of the probability of neutron, proton, and α -particle emission was performed both in equilibrium, and in the pre-equilibrium stages of the process. Fission and γ -ray emission were also considered after equilibration. The analysis of the experimental data on the double-differential cross sections of p, α particles for the $^{16}\text{O} + ^{116}\text{Sn}$ reaction at the oxygen energy $E = 130$ and 250 MeV were performed.

1. INTRODUCTION

Now new experimental data of the double-differential spectra of light particles emitted at pre-equilibrium stage of nuclear reactions are known. This data was measured using the GARFIELD apparatus [1] in coincidence with evaporation residues for the 130 and 250 MeV $^{16}\text{O} + ^{116}\text{Sn}$ reaction. In this connection a study of the process of compound nuclear de-excitation is impossible without taking into account the nonequilibrium mechanism of particle emissions and the calculations of the nonequilibrium double-differential spectra are of importance. To analyze the effect of nonequilibrium processes on the particle emission we used a traditional approximation where one should distinguish conventionally two steps: pre-equilibrium and evaporation. The compound nuclear system achieves equilibrium either after emission of one pre-equilibrium particle or after establishment of thermodynamic equilibrium. In the first approach we used the Griffin's exciton model of the nonequilibrium processes [2, 3]. The equilibrium

evaporation process was analyzed in the framework of the statistical theory of nuclear reactions with Monte-Carlo simulation including certain dynamical and kinematical characteristics. The PACE code was modified [4, 5] for the calculations of pre-equilibrium process at excitation energies of hundreds MeV. In this work the theoretical description was compared with the experimental spectra for protons and α particles. Special attention is paid to the angular dependence of the pre-equilibrium particle spectra.

2. METHOD OF THE ANALYSIS

The main assumption in the models of pre-equilibrium processes is that the incident beam loses its energy gradually. Thus, a distinction can be made after each collision between the fast particle and the nucleons excited by the collision from states below the Fermi energy. Let n be the number of excitons (i.e., particles and holes, including the fast particle). In the Griffin's exciton model [2] of nuclear reactions, relaxation of the composite nuclear system to equilibrium is described by the master equation:

$$\frac{d}{dt}q(n, t) = \sum_{m=n-2}^{m=n+2} \lambda_{m \rightarrow n} q(m, t) - q(n, t) \left(w(n) + \sum_{m=n-2}^{m=n+2} \lambda_{n \rightarrow m} \right), \quad (1)$$

where $q(n, t)$ is the occupation probability for the composite nucleus state n , $w(n)$ is the emission rate

¹⁾D. V. Skobel'syn Institute of Nuclear Physics, Moscow State University, Russia.

²⁾Istituto Nazionale di Fisica Nucleare, Laboratori Nazionali di Legnaro (Pd), Italy.

³⁾Dipartimento di Fisica dell'Università di Bologna, Italy.

⁴⁾Istituto Nazionale di Fisica Nucleare, Sezione di Firenze, Italy.

⁵⁾Istituto Nazionale di Fisica Nucleare, Sezione di Bologna, Italy.

⁶⁾Istituto Nazionale di Fisica Nucleare, and Dipartimento di Fisica dell'Università di Milano, Italy.

*E-mail: fotina@srd.sinp.msu.ru

of light particles (in our case — neutrons, protons and α particles), $\lambda_{m \rightarrow n}$ is the internal transition rate. The positive terms at the right-hand side of Eq. (1) describe the feeding to the state n from all possible states m , and the negative terms account for the losses of the system due to emission and transitions to other exciton states. The internal transition rates, $\lambda_{m \rightarrow n}$, are determined by the matrix element of the transitions, $\langle |M|^2 \rangle$, and the densities of the exciton states to that the transitions occur, $\omega_{0,\pm}(n, E)$. In the model the densities of the exciton states are determined by the single-particle level density g . The last one is related with the level density parameter of the Fermi-gas model a . For these parameters we used the same values as in the evaporation case. The details of the transition rate calculations used in our approach can be found in [6].

We regard as free parameters the following values: n_0, k, g . k is a parameter connected with the transition matrix element $\langle |M|^2 \rangle$. It determines the transition rate of the emitted particle into continuum. This parameter was varied in wide range from 200 to 800 MeV³. The single-particle level density g (which is used to determine the densities of exciton states) is connected with the level density parameter in the Fermi-gas model by the relation $g = 6a/\pi^2$. The a parameter was chosen in the framework of the Fermi-gas model or the level-density phenomenological model (see [7]) with the Grudzevich parameterization (see [8]). n is the exciton number mentioned above. The initial exciton configuration $n_0 = p_0 + h_0$ from which the equilibration process starts. It is a free parameter of the model. In our calculations we used the following initial exciton configuration: $n_0 = (16p, 1h)$ (for the $^{16}\text{O} + ^{116}\text{Sn}$ reaction).

It should be noticed that the equilibrium emission of light particles (neutrons, protons, and α particles) and γ quanta was considered in the framework of the Hauser–Feshbach formalism (see, e.g., [9]). To calculate transmission coefficients the optical model was used with the parameters for the α particles from [10], for protons — from [11], and for neutrons — from [12]. The fission decay widths were calculated in an ordinary way as provided by the PACE code.

In the frame of Griffin model we calculated the equilibrium and pre-equilibrium particle ejection probabilities and the energy spectra of pre-equilibrium particles (neutrons, protons, and α particles). In the following step using Monte-Carlo simulations we obtained the kind of pre-equilibrium particle (neutron, proton, or α particle) with its energy. Using the optical model we determined the angular momentum of the emitted particles. On the first step of our investigations for the pre-equilibrium particles we used some model distribution of angular

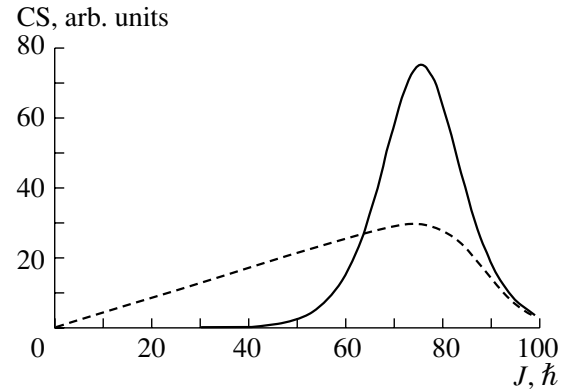


Fig. 1. Distribution of Cross Section (CS) over angular momentum (J) for evaporation particles (dashed curve) and nonequilibrium particles (solid curve).

moments. For the certain angular momentum values we estimated the particle ejection angles in the framework of the standard PACE procedure using the corresponding associated Legendre functions. For example, in Fig. 1 we present two cases of the angular momentum distributions for evaporation particles and nonequilibrium particles with equal values of the ejection cross section.

3. RESULTS AND DISCUSSION

Below we show the results of the calculations of the equilibrium together with the pre-equilibrium double-differential spectra of light particles (protons and α particles, Figs. 2–5) from the $^{16}\text{O} + ^{116}\text{Sn}$ reaction for the oxygen energy 130 and 250 MeV. Experimental data for protons and α particles are presented also.

The experimental data were collected using the GARFIELD (General ARray of Fragment Identification and for Emitted Light particles in Dissipative collisions) apparatus [1] at the Legnaro National Laboratory (Italy). The results under discussion concern proton and α particle emission for the 130- and 250-MeV $^{16}\text{O} + ^{116}\text{Sn}$ reactions. Pulsed beams (around 1 ns FWHM) of ^{16}O provided by the TANDEM–ALPI acceleration system were used to bombard ^{116}Sn targets 500 $\mu\text{g}/\text{cm}^2$ thick. In case of complete fusion this reaction leads to the compound nucleus ^{132}Ce , with excitation energies of 100 and 200 MeV for two oxygen energies, respectively. The GARFIELD is azimuthally divided into 24 sectors, and each sector consists of eight ΔE – E telescopes for a total of 192 telescopes covering an angular range from $\theta = 29^\circ$ to $\theta = 82^\circ$ and 2π in ϕ . Evaporation

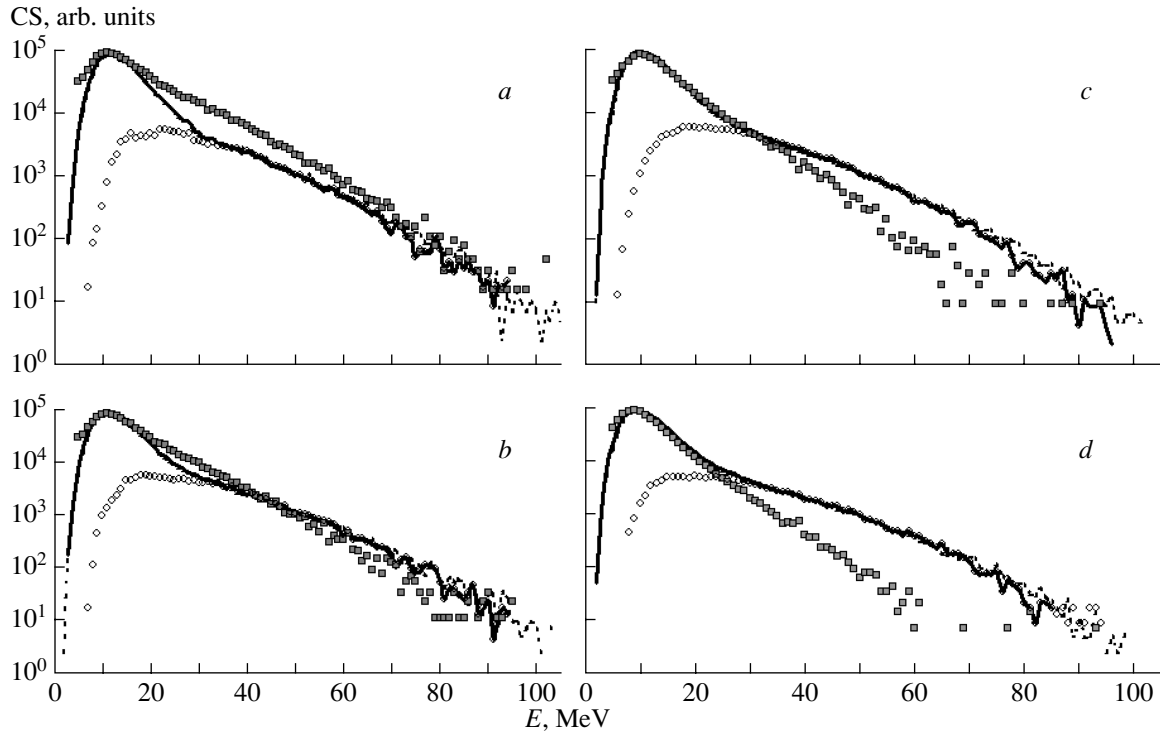


Fig. 2. Double-differential spectra (CS) for protons for the oxygen energy $E = 250$ MeV. Dashed curve corresponds $P_\alpha = 0$, solid curve corresponds $P_\alpha = 0.5$. Open circles show the pre-equilibrium part of spectrum. Experimental data are shown by the squares. Angular ranges are: (a) $29^\circ\text{--}41^\circ$, (b) $41^\circ\text{--}53^\circ$, (c) $53^\circ\text{--}67^\circ$, (d) $67^\circ\text{--}83^\circ$.

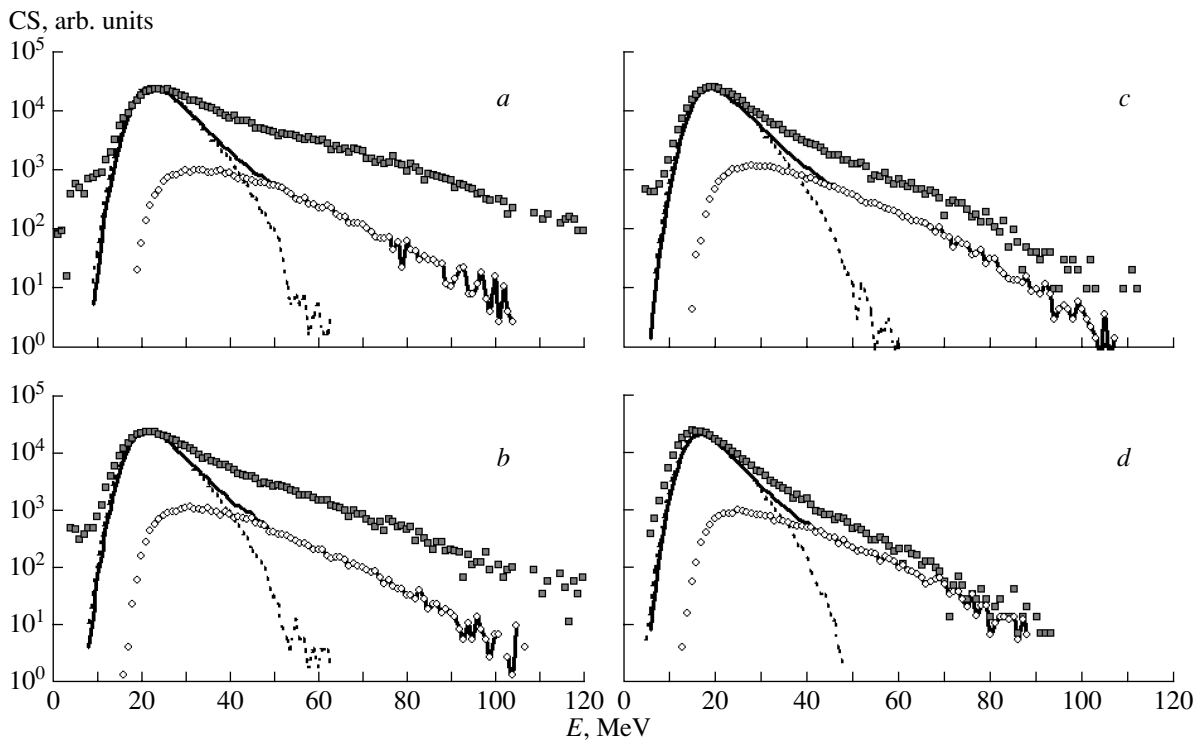


Fig. 3. Double-differential spectra (CS) for α particles for the oxygen energy $E = 250$ MeV. Symbols, curves, and angular ranges are the same as in Fig. 2.

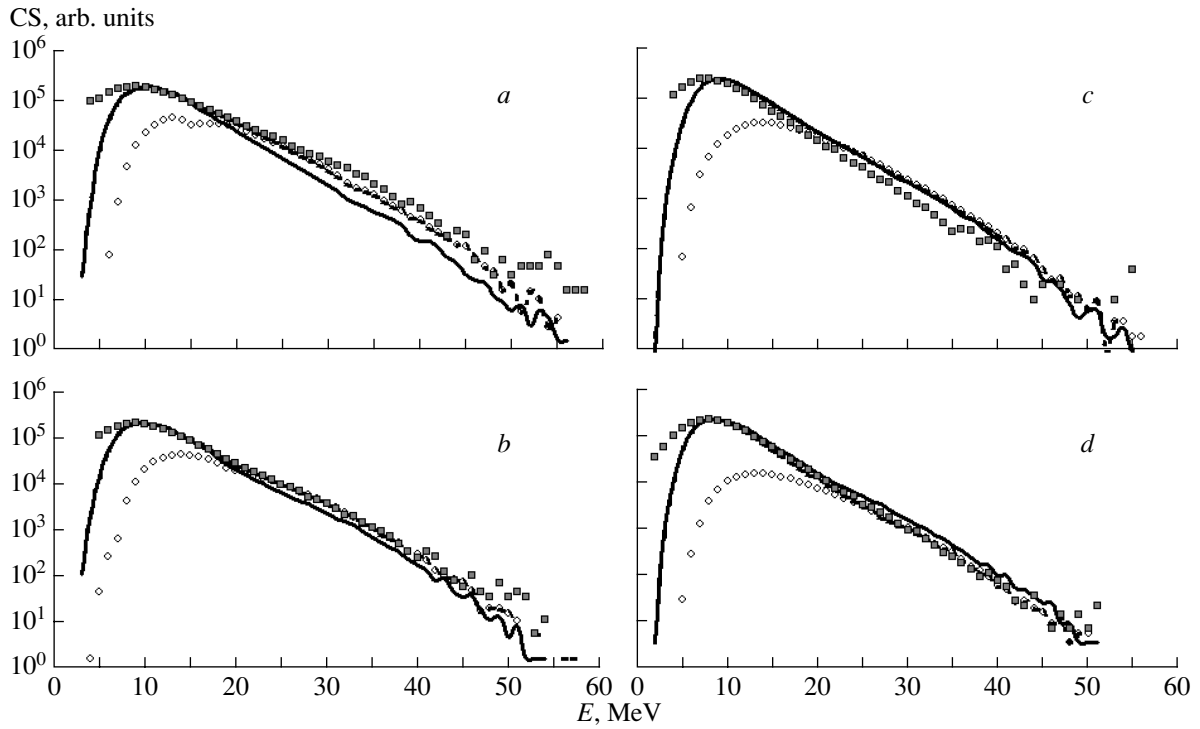


Fig. 4. Double-differential spectra (CS) for protons for the oxygen energy $E = 130$ MeV. Solid curve corresponds case *A* (see text), dashed curve corresponds case *B*. Open circles show the pre-equilibrium part of spectrum for case *B*. Experimental data are shown by the squares. Angular ranges are the same as in Fig. 2.

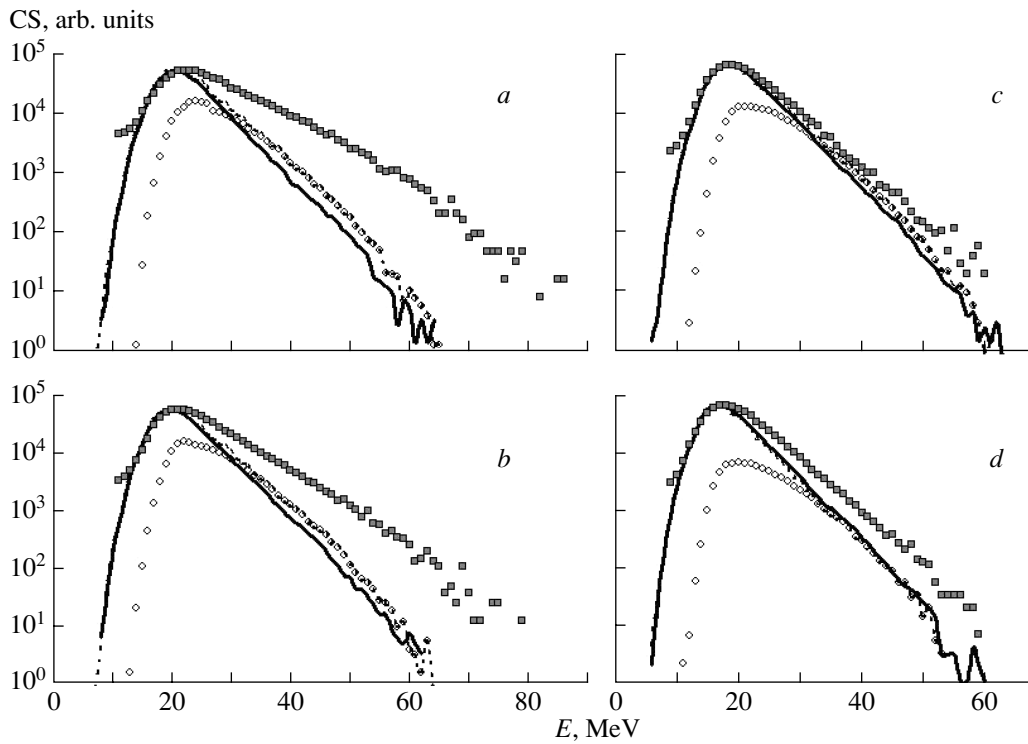


Fig. 5. Double-differential spectra (CS) for α particles for the oxygen energy $E = 130$ MeV. Symbols, curves are the same as in Fig. 4; angular ranges are the same as in Fig. 2.

residues produced in the reactions have been detected using two couples of Position Sensitive Parallel Plate Avalanche Counters. The light charged particles were measured in coincidence with evaporation residues. For more details see [13].

The double-differential spectra for protons (Figs. 2, 4) and α particles (Figs. 3, 5) from the $^{16}\text{O} + ^{116}\text{Sn}$ reaction are presented. We show the results for the same four angles as in the experiments. Angular ranges in Figs. 3–5 are: for $a - 29^\circ - 41^\circ$; for $b - 41^\circ - 53^\circ$; for $c - 53^\circ - 67^\circ$; for $d - 67^\circ - 83^\circ$. Experimental data are shown as squares. Data for the oxygen energy $E = 250$ MeV are presented in Figs. 2, 3. Data for the oxygen energy $E = 130$ MeV are in Figs. 4, 5.

Figures 2, 3 show two cases for the simulation of the nonequilibrium process. The first one is the case when preformation probability of α particles equals zero $P_\alpha = 0$. The similar assumptions are usually used in the coalescence model, see [14]. The second one is the case when $P_\alpha \neq 0$ [15]. In our estimations we used P_α value as a free parameter. Variation of this value influences α -particle spectra very strongly (Fig. 3). But influence of this coefficient on proton spectra is not so pronounced (Fig. 3). Note that with $P_\alpha = 0$ the description of experimental data on double differential spectra for α particles is not possible. It indicates that the probability of the α -cluster preformation in the target nuclei is not zero and this processes is important.

In Figs. 3, 4 the same data are presented for the oxygen energy $E = 130$ MeV. For comparison we present the results of estimations performed in the framework of Griffin model (Case A) and the hybrid exciton model with the generalized master equation [16, 17] (Case B). The results in the Case B demonstrate the better description of the nonequilibrium part of the particle emission spectra. One should notice also the good agreement for protons between the experimental data and the theoretical predictions of the Griffin model (Fig. 4) for these angular ranges for $E = 130$ MeV. So, even simple exciton model provides a good description of the angular dependence for the nonequilibrium proton spectra for this energy. On the contrary, for α particles the situation is not so good. Moreover one can see that the difference between the experimental and the calculation results grows for more forward angles for both energies of the oxygen projectile: 130 and 250 MeV. This effect seems to be associated with the α -cluster structure of the oxygen projectile (see [18]).

4. CONCLUSIONS

Experimental data on the nonequilibrium particle emission provides an interesting input for the theoretical models. It was demonstrated that the Griffin

exciton model describes satisfactorily the nonequilibrium proton spectra.

Nevertheless, for the description of secondary α -particle spectra from the reactions induced by the ^{16}O projectile, we found that it is very important to take into account the probability of α -particle preformation in the target nuclei and eventually in the projectile (α clustering).

We plan to measure the same experimental information in the reactions induced by projectiles with different probabilities of α clusterization (for example, oxygen- and fluorine-induced reactions). It is expected that the theoretical analysis of this experimental data will allow us to extract information on the probability of α -particle pre-formation in the projectile.

REFERENCES

1. F. Gramegna *et al.*, Nucl. Instrum. Methods A **389**, 474 (1997).
2. J. J. Griffin, Phys. Rev. Lett. **17**, 478 (1966).
3. D. O. Eremenko, S. Yu. Platonov, O. V. Fotina, and O. A. Yuminov, Phys. At. Nucl. **61**, 695 (1998).
4. I. M. Egorova *et al.*, Bull. Rus. Acad. Sci. Phys. **66**, 1622 (2002).
5. D. O. Eremenko, O. V. Fotina, G. Giardina, *et al.*, Phys. At. Nucl. **65**, 18 (2002).
6. Yu. L. Parfenova, O. V. Fotina, and Yu. A. Yuminov, Bull. Rus. Acad. Sci. Phys. **63**, 758 (1999).
7. A. V. Ignatyuk, K. K. Istekov, and G. N. Smirenkin, Sov. J. Nucl. Phys. **29**, 450 (1979).
8. O. T. Grudzevich *et al.*, Radiat. Protect. Dosim. **126**, 101 (2007).
9. W. Hauser and H. Feshbach, Phys. Rev. **87**, 366 (1952).
10. J. R. Huizenga and G. Igo, Nucl. Phys. **29**, 462 (1962).
11. F. G. Perey, Phys. Rev. **131**, 745 (1963).
12. D. Wilmore and P. E. Hodgson, Nucl. Phys. **55**, 673 (1964).
13. V. L. Kravchuk, S. Barlini, and O. V. Fotina, Eur. Phys. J., to be published.
14. T. C. Awes, S. Saini, G. Poggi, *et al.*, Phys. Rev. C **25**, 2361 (1982).
15. R. Bonetti, L. M. Colli, and G. D. Sassi, J. Phys G **3**, 1111 (1977).
16. G. Mantzouranis, H. A. Weidenmuller, and D. Agassi, Z. Phys. A **276**, 145 (1976).
17. J. M. Akkermans, H. Gruppelaar, and G. Reffo, Phys. Rev. C **22**, 73 (1980).
18. Yu. A. Berezhnoy and V. P. Mikhailyuk, Phys. Part. Nucl. **39**, 221 (2008).

ДВАЖДЫ ДИФФЕРЕНЦИАЛЬНЫЕ СПЕКТРЫ ВТОРИЧНЫХ ЧАСТИЦ В РАМКАХ ПРЕДРАВНОВЕСНОЙ МОДЕЛИ

**О. В. Фотина, В. Л. Кравчук, С. Барлини, Ф. Граменья, Д. О. Еременко, Ю. Л. Парфенова,
С. Ю. Платонов, О. А. Юминов, М. Бруно, М. Д'Агостино, Дж. Касини, О. Виеланд,
А. Бракко, А. Камера**

Развит подход для описания дважды дифференциальных спектров вторичных частиц, образующихся в результате реакций на средних и тяжелых ионах. Для учета неравновесной стадии процесса образования составной системы используется простая модель Гриффина предравновесных процессов. Моделирование процессов девозбуждения составной системы проводится с использованием метода Монте-Карло. Как на равновесной, так и на предравновесной стадии процесса анализируется вероятность испускания нейтронов, протонов и α -частиц. После установления равновесия в процессе девозбуждения дополнительно учитывается возможность деления и испускания γ -квантов. В качестве примера выполнен анализ экспериментальных данных по дважды дифференциальным сечениям протонов и α -частиц для реакции $^{16}\text{O} + ^{116}\text{Sn}$ при энергии налетающего кислорода $E = 130$ и 250 МэВ.